Nonlinear Dyn (2017) 88:1643–1653
DOI 10.1007/s11071-017-3336-1

ORIGINAL PAPER

Application of subharmonic resonance for the detection of bolted joint looseness

Mengyang Zhang · Yanfeng Shen · Li Xiao · Wenzhong Qu

Received: 17 November 2015 / Accepted: 3 January 2017 / Published online: 9 January 2017

Abstract Bolted joint structures are prone to bolt loosening under environmental and operational vibrations, which may severely affect the structural integrity. This paper presents a bolt looseness recognition method based on the subharmonic resonance analysis. The bolted joint structure was simplified to a two-degree-of-freedom nonlinear model, and a multiple timescale method was used to explain the phenomenon of the subharmonic resonance and conditions for the generation of subharmonics. Numerical simulation predictions for the generation of the subharmonics and conditions for the subharmonics can be found with respect to the excitation frequency and the excitation amplitude. Experiments were performed on a bolt-joint aluminum beam, where the damage was simulated by loosening the bolts. Two surface-bonded piezoelectric transducers were utilized to generate continuous sinusoidal excitation and to receive corresponding sensing signals. The experimental results demonstrated that subharmonic components would appear in the response spectrum when the bolted structure was subjected to the excitation of twice its natural frequency. This subharmonic resonance method was found to be effective on bolt looseness detection.

Keywords Bolt looseness detection · Structural health monitoring · Subharmonic · Method of multiple scales · Piezoelectric transducers

1 Introduction

Bolted joints are widely used in construction and mechanical industries to connect bear loading structures, and the loss of torque in one or more bolts can dramatically reduce the fatigue life of the mechanical parts [1]. For this reason, a quick assessment of the health status of bolted joints would elongate structural service life spans and prevent catastrophic failures in a variety of mechanical applications.

Among various inspection methods, nonlinear acoustic/ultrasonic techniques are drawing increasing attention within the structural health monitoring (SHM) community, due to their high sensitivity to incipient damage with distinctive nonlinear signal features [2]. In general, the appearance of contact surfaces in the wave paths contributes a significant increase in acoustic nonlinearity [3]. When a bolt becomes loose, a variation of contact stiffness at the interface exists under cyclic wave/vibration loading [4]. Several approaches have been investigated for the detection of bolt loosening, such as impedance method, electrical conductivity approach, and via vibration measurements [5–8]. Elastic waves propagating through the loosening bolted

M. Zhang · L. Xiao · W. Qu (✉)
Department of Engineering Mechanics, Wuhan University, Wuhan 430072, China
e-mail: qwz@whu.edu.cn

Y. Shen
University of Michigan-Shanghai Jiao Tong University Joint Institute, Shanghai Jiao Tong University, 800 Dongchuan Road, Shanghai 200240, China

joints will be distorted, due to the existence of contact interfaces, showing the contact acoustic nonlinearity (CAN), which may produce a completely different signal feature compared to the source excitation. This signal carries information about the structural nonlinearity, present in the form of higher harmonics. Moreover, the amplitude ratio between the fundamental frequency and second harmonic component may serve as an important parameter as the measurement of structural nonlinearity [9]. Some other authors quantified torque loss in bolted joints through the magnitudes of the side-band response [10,11]. It has been widely reported that the generation of higher harmonics is a promising technique for monitoring the health state of the bolted joint structures. Its superb sensitivity is a benefit for incipient damage detection, but may also result in a wide range of uncertainty and unreliability [12]. For example the electronic equipment will also bring higher-harmonic components in the measurements, i.e., the signal directly from a function generator already carries inherent higher harmonics due to the nonlinear electronic system. Such situation is inevitable and usually causes considerable difficulties and even false alarms in the practical applications of higher-harmonic techniques. Subharmonics, on the other hand, cannot be introduced by electronic equipment and their generation requires specific conditions, which makes them more reliable for bolted joint loosening detection. On the study of subharmonic resonance phenomena, Ohara et al. [13] introduced a breathing crack model and conducted the experiments for crack detection using the subharmonic array. Johnson et al. [14] developed a single- degree-of-freedom mass–spring oscillator with bilinear stiffness and adopted a finite element model of a cracked rod to verify the theoretical exciting frequency condition of subharmonic component. Mahmoodi et al. [15] derived the subharmonic resonance in nonlinear flexural vibrations of a piezoelectrically actuated micro-cantilever using the multiple scales method, verified by experiments.

To date, most nonlinear vibration/ultrasonic techniques are focused on higher-harmonic and side-band modulation methods, but nonlinear damage detection approaches based on subharmonic resonance still require more investigation, especially for bolt looseness detection. In this study, a subharmonic method with the anti-interference advantage is proposed for the detection of bolt looseness. We will first illuminate the development of a 2-DOF nonlinear model to analyze the physical phenomenon of subharmonics and their generation conditions. Numerical solutions and case studies will be shown to understand the subharmonic effects. Experiments are finally performed on a bolted aluminum beam, and the experimental results demonstrate the validity and effectiveness of the proposed subharmonic resonance method.

2 Theoretical analysis

In this study, we adopted a reduced-order 2-DOF nonlinear model to derive and understand the generation condition of subharmonic resonances which serves as a general predictive model for nonlinear contact dynamics between structural interfaces. This model consists of two masses which are coupled by a nonlinear restoring force F_N, as shown in Fig.1. The model is excited

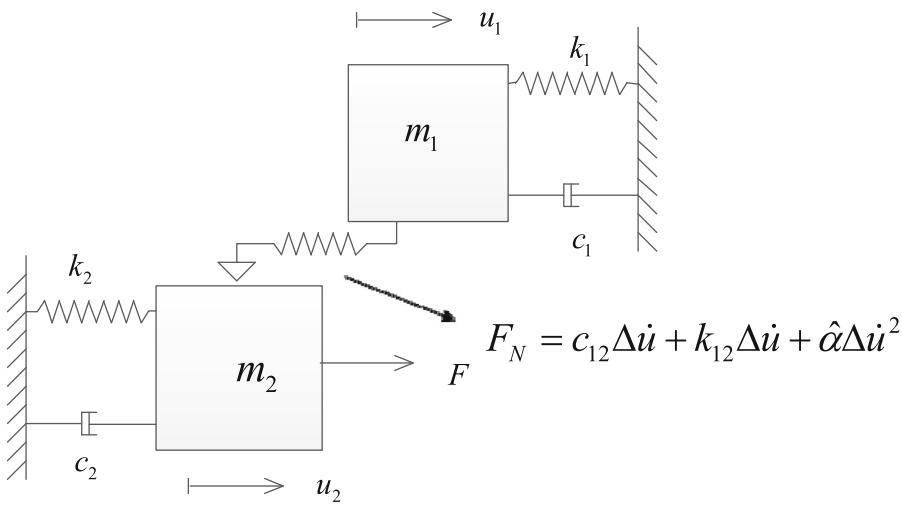

Fig. 1 Schematic of the 2-DOF nonlinear model with second- order polynomial restoring forces

at the mass m_2. u_1, u_2 are the displacements of m_1, m_2, respectively. Such a 2-DOF nonlinear model was first introduced by Bograd et al. [16] as a simple mechanical system with a node-to-node contact. In that case, the harmonic balance method (HBM) was used to linearize nonlinear restoring force resulting equivalent stiffness and damping. In general, it is very hard to conclude a close-form solution for the frequency response of the assembled beam with nonlinear joint interface properties. To have a better understanding of subharmonic resonance on bolted joints and the particular conditions on the input signal to trigger this nonlinear effect, the restoring force F_N can be written as a second-order polynomial of the relative displacement Δu, i.e., $F_N = c_{12}\Delta\dot{u} + k_{12}\Delta u + \hat{\alpha}\Delta\dot{u}^2$, where $\Delta u = u_1 - u_2$ and a viscous damper represents the energy dissipation at the joint; a choice of a quadratic spring force was rationalized based on the experimental results. First, both superharmonic components and DC term exist in the response of any kind of excitation form in the following experiment. Second, other bolt looseness detection method like the impact modulation shows that sidebands in impact modulation experiment data occurred at frequencies equal to the probing frequency plus and minus the natural frequencies [17]. These phenomena imply the existence of a quadratic spring force. The equation of motion for this model is thus given by:

$$\begin{cases} m_1\ddot{u}_1 + c_1\dot{u}_1 + k_1u_1 + F_N = 0 \\ m_2\ddot{u}_2 + c_2\dot{u}_2 + k_2u_2 - F_N = F\cos\omega t. \end{cases} \tag{1}$$

where m_1, m_2 are the masses; k_1, k_2, k_{12} denote the linear stiffness of the system; c_1, c_2, c_{12} represent damping terms; $\hat{\alpha}$ is the coefficient of the quadratic term; and F and ω are the amplitude and frequency of a harmonic excitation, respectively.

Arranging Eq. (1) in matrix form yields

$$\begin{bmatrix} m_1 & 0 \\ 0 & m_2 \end{bmatrix}\begin{pmatrix} \ddot{u}_1 \\ \ddot{u}_2 \end{pmatrix} + \begin{bmatrix} c_1 + c_{12} & -c_{12} \\ -c_{12} & c_{12} + c_2 \end{bmatrix}\begin{pmatrix} \dot{u}_1 \\ \dot{u}_2 \end{pmatrix} + \begin{bmatrix} k_1 + k_{12} & -k_{12} \\ -k_{12} & k_{12} + k_2 \end{bmatrix}\begin{pmatrix} u_1 \\ u_2 \end{pmatrix} = \begin{Bmatrix} -\hat{\alpha}(u_1 - u_2)^2 \\ \hat{\alpha}(u_1 - u_2)^2 + F\cos\omega t \end{Bmatrix}. \tag{2}$$

From Eq. (2), we can obtain the equations of motion for the corresponding undamped linear system as

$$\begin{bmatrix} m_1 & 0 \\ 0 & m_2 \end{bmatrix}\begin{pmatrix} \ddot{u}_1 \\ \ddot{u}_2 \end{pmatrix} + \begin{bmatrix} k_1 + k_2 & -k_{12} \\ -k_{12} & k_1 + k_2 \end{bmatrix}\begin{pmatrix} u_1 \\ u_2 \end{pmatrix} = 0. \tag{3}$$

In this way, two natural frequencies of this linear system can be identified

$$\omega_{1,2}^2 = \frac{k_{12}m_1 + k_{12}m_2 + k_1m_2 + k_2m_1 \pm \sqrt{(k_{12}m_1 + k_{12}m_2 + k_1m_2 + k_2m_1)^2 - 4(k_1k_2 + k_{12}k_1 + k_{12}k_2)m_1m_2}}{2m_1m_2}.$$

The main vibration modes of the linear system are

$$\phi = \begin{pmatrix} \phi_1 & \phi_2 \end{pmatrix} = \begin{pmatrix} \frac{k_{12}+k_2-\omega_1^2m_1}{k_{12}} & \frac{k_{12}+k_2-\omega_2^2m_1}{k_{12}} \\ 1 & 1 \end{pmatrix}. \tag{4}$$

In order to simplify the derivation, it is assumed that $k_1 = k_2 = k_{12} = k$, $m_1 = m_2 = m$, $c_1 = c_2 = c_{12} = c$, then $\omega_1^2 = \frac{3k}{m}, \omega_2^2 = \frac{k}{m}, \phi = \begin{pmatrix} -1 & 1 \\ 1 & 1 \end{pmatrix}$.

The normal modal shapes are $\Psi = \frac{1}{\sqrt{m_i}}, \phi = \frac{1}{\sqrt{2m}}\begin{pmatrix} -1 & 1 \\ 1 & 1 \end{pmatrix}$. Performing the change of variables $u = \Psi x$, Eq. (2) takes the following non-dimensional form:

$$\begin{bmatrix} 1 & 0 \\ 0 & 1 \end{bmatrix}\begin{pmatrix} \ddot{x}_1 \\ \ddot{x}_2 \end{pmatrix} + \begin{bmatrix} 2\hat{\mu}_1 & 0 \\ 0 & 2\hat{\mu}_2 \end{bmatrix}\begin{pmatrix} \dot{x}_1 \\ \dot{x}_2 \end{pmatrix} + \begin{bmatrix} \omega_1^2 & 0 \\ 0 & \omega_2^2 \end{bmatrix}\begin{pmatrix} x_1 \\ x_2 \end{pmatrix} = \begin{Bmatrix} \hat{\alpha}\frac{2}{m}\sqrt{\frac{2}{m}}x_1^2 + f\cos\omega t \\ f\cos\omega t \end{Bmatrix}. \tag{5}$$

where $\hat{\mu}_1 = \frac{3c}{2m}$, $\hat{\mu}_2 = \frac{c}{2m}$, and $f = \frac{1}{\sqrt{2m}}F$.

The method of multiple timescales as presented in Ref. [18] can be applied to solve Eq. (5). This method uses multiple timescales T_0, T_1 as independent variables, which stand for the fast and slow timescales, respectively. The solutions for x are assumed of the following forms:

$$\begin{aligned} x_1(t,\varepsilon) &= x_{11}(T_0, T_1) + \varepsilon x_{12}(T_0, T_1), \\ x_2(t,\varepsilon) &= x_{21}(T_0, T_1) + \varepsilon x_{22}(T_0, T_1). \end{aligned} \tag{6}$$

The coefficients of the nonlinear term and damping are scaled as $\hat{\mu} = \varepsilon\mu, \hat{\alpha} = \varepsilon\alpha$, where ε is a small parameter which indicates that the damping and nonlinearity are weak. The time dependence is expanded into multiple timescales as:

$$t = T_0 + \varepsilon T_1 + \cdots, \tag{7}$$

$$\frac{d()}{dt} = \frac{dT_0}{dt}\frac{\delta()}{\delta T_0} + \frac{dT_1}{dt}\frac{\delta()}{\delta T_1} + \cdots = D_0 + \varepsilon D_1 + \cdots. \tag{8}$$

Substituting Eq. (8) into Eq. (5), the coefficients of ε at orders ε^0 and ε^1 are then equated to give:

ε^0:

$$D_0^2 x_{11} + \omega_1^2 x_{11} = f\cos\omega t, \tag{9}$$

$$D_0^2 x_{21} + \omega_2^2 x_{21} = f\cos\omega t. \tag{10}$$

ε^1:

$$D_0^2 x_{12} + \omega_1^2 x_{12} = -2D_0 D_1 x_{11} + \frac{2}{m}\sqrt{\frac{2}{m}}\alpha x_{11}^2 - 2\mu_1 D_0 x_{11}, \tag{11}$$

$$D_0^2 x_{22} + \omega_2^2 x_{22} = -2D_0 D_1 x_{21} - 2\mu_2 D_0 x_{21}. \tag{12}$$

The general solution of Eqs. (9) and (10) is:

$$x_{11} = A_1 e^{i\omega_1 T_0} + \Lambda_1 e^{i\omega T_0} + c.c., \tag{13}$$

$$x_{21} = A_2 e^{i\omega_2 T_0} + \Lambda_2 e^{i\omega T_0} + c.c., \tag{14}$$

where c.c. stands for the complex conjugate of the previous terms; A_1, A_2 stand for the complex amplitude of free vibration; and Λ_1, Λ_2 match the forced response of a linear system. The value of Λ_1, Λ_2 is easily obtained by combining similar terms; therefore, $\Lambda_1 = \frac{f}{2(\omega_1^2-\omega^2)}$ and $\Lambda_2 = \frac{f}{2(\omega_2^2-\omega^2)}$. It can be seen that the resonance term of x_1 and x_2, respectively, appears in the transient response besides the forced response.

Substituting Eqs. (13) and (14) into Eqs. (11) and (12):

$$\begin{aligned} &D_0^2 x_{12} + \omega_1^2 x_{12} = -2i\omega_1 A_1' e^{i\omega_1 T_0} \\ &+\frac{2}{m}\sqrt{\frac{2}{m}}\alpha(A_1^2 \mathrm{e}^{2i\omega_1 T_0} + \Lambda_1^2 \mathrm{e}^{2i\omega T_0} + 2A_1\Lambda_1 \mathrm{e}^{i(\omega_1+\omega)T_0} \\ &+2A_1\bar{\Lambda}_1 \mathrm{e}^{i(\omega_1-\omega)T_0} \\ &+A_1\bar{A}_1 + \Lambda_1\bar{\Lambda}_1) - 2\mu_1(A_1 i\omega_1 \mathrm{e}^{i\omega_1 T_0} \\ &+\Lambda_1 i\omega \mathrm{e}^{i\omega T_0}) + c.c., \end{aligned} \tag{15}$$

$$\begin{aligned} &D_0^2 x_{22} + \omega_2^2 x_{22} = -2i\omega_2 A_2' e^{i\omega_2 T_0} \\ &-2\mu_2(A_2 i\omega_2 \mathrm{e}^{i\omega_2 T_0} + \Lambda_2 i\omega \mathrm{e}^{i\omega T_0}) + c.c., \end{aligned} \tag{16}$$

where the prime denotes differentiation with respect to T_1 and the overbar denotes the complex conjugate. In this case, all secular terms having factor $\mathrm{e}^{i\omega_1 T_0}$ in Eq. (15) and factor $\mathrm{e}^{i\omega_2 T_0}$ in Eq. (16) should be set to zero to obtain Eqs. (17) and (18). By introducing a small detuning parameter σ, which allows the frequency to vary slightly from the resonance and set $\omega = 2\omega_1 + \varepsilon\sigma$ to give:

$$-i\omega_1 A_1' + \beta A_1\bar{\Lambda}_1 e^{i\sigma T_1} - \mu_1 A_1 i\omega_1 = 0, \tag{17}$$

where $\beta = \frac{2}{m}\sqrt{\frac{2}{m}}\alpha$.

$$2i\omega_2 A_2' + 2\mu_2 A_2 i\omega_2 = 0. \tag{18}$$

Equation (18) is a first-order ordinary differential equation and can be easily solved for the function $A_2 = \mathrm{C}e^{-\mu_2 T_1}$, where C is a constant which can be determined form the initial conditions of the system. This solution shows that A_2 will decay away over time. Therefore, the response of x_2 will only contain the frequency content at the excitation frequency ω. To solve Eq. (17) for function A_1, a function $B(T_1)$ is defined, such that

$$A_1(T_1) = B(T_1)e^{\frac{1}{2}i\sigma T_1}. \tag{19}$$

This solution shows that the complex amplitude A_1 varies with T_1, which indicates whether A_1 will be decay away over time depending on the complex amplitude $B(T_1)$. Separating $B(T_1)$ into its real and imaginary components, i.e., $B = B_r + iB_i$, applying Eq. (19) to Eq. (17), and setting the real and imaginary portions of the result to zero independently will lead to the following two equations expressed in matrix form:

$$\begin{pmatrix} B_r' \\ B_i' \end{pmatrix} = \begin{pmatrix} -\mu_1 & \frac{\sigma}{2} - \frac{\beta\Lambda_1}{\omega_1} \\ -\frac{\sigma}{2} - \frac{\beta\Lambda_1}{\omega_1} & -\mu_1 \end{pmatrix} \begin{pmatrix} B_r' \\ B_i' \end{pmatrix}. \tag{20}$$

Assuming the solution $\begin{pmatrix} B_r \\ B_i \end{pmatrix} = \begin{pmatrix} b_r \\ b_i \end{pmatrix} e^{\lambda T_1}$, where b_r, b_i, and λ are constants, we will arrive at the following eigenvalue problem:

$$\begin{pmatrix} b_r \\ b_i \end{pmatrix}\lambda = \begin{pmatrix} -\mu_1 & \frac{\sigma}{2} - \frac{\beta\Lambda_1}{\omega_1} \\ -\frac{\sigma}{2} - \frac{\beta\Lambda_1}{\omega_1} & -\mu_1 \end{pmatrix} \begin{pmatrix} b_r \\ b_i \end{pmatrix}. \tag{21}$$

The eigenvalues $\lambda = -\mu_1 \pm \sqrt{-\frac{\sigma^2}{4} + \frac{\beta^2\Lambda_1^2}{\omega_1^2}}$.

Thus, the approximate solution for x_{12} is:

$$\begin{aligned} x_{12} = {} & \varphi_1 e^{i\omega_1 T_0} + \varphi_2 e^{2i\omega_1 T_0} + \varphi_3 e^{2i\omega T_0} + \varphi_4 e^{i(\omega_1+\omega)T_0} \\ & + \varphi_5 A\bar{A} + \varphi_6\Lambda_1\bar{\Lambda}, \end{aligned} \tag{22}$$

where $\varphi_1 = \frac{2i\mu_1\Lambda\omega}{\omega^2-\omega_1^2}$, $\varphi_2 = \frac{\beta A_1^2}{3\omega_1^2}$, $\varphi_3 = \frac{\beta\Lambda_1^2}{4\omega^2-\omega_1^2}$, $\varphi_4 = \frac{2\beta\bar{A}\Lambda}{(\omega+\omega_1)^2-\omega_1^2}$, $\varphi_5 = \varphi_6 = \frac{\beta}{\omega_1^2}$.

These expressions give a theoretical amplitude relationship between the frequency contents, from which we can know there is more than one frequency component in the response signal, unlike linear systems. In linear damping systems, natural frequency resonance can only exist in transient response. In nonlinear systems, free response component, oscillating at natural frequency ω_1 known as a 1:2 subharmonic, will not decay away over time, if λ has one positive eigenvalue. Thus, the following condition must be satisfied:

$$\mu_1 < \sqrt{-\frac{\sigma^2}{4} + \frac{\beta^2\Lambda_1^2}{\omega_1^2}}. \tag{23}$$

In an alternative form, we can express this condition with respect to the excitation amplitude:

$$F > \frac{m^2\omega_1(\omega^2-\omega_1^2)}{\alpha}\sqrt{\frac{(\omega-2\omega_1)^2}{4}+\mu_1^2}. \tag{24}$$

Hence, we arrive at the threshold condition of subharmonic generation. In satisfying this condition, we have known that external forcing frequency must be near twice the natural frequency and the forcing amplitude must exceed some value determined by parameters μ_1, ω_1, α. This threshold condition is crucial for the proper choice of excitation frequency and amplitude to trigger subharmonic resonance effect, so that we can make effective use of it for nonlinear damage detection.

3 Numerical solutions

In order to study the generation of subharmonics in the nonlinear model, Eq. (5) was solved using MATLAB with a sampling frequency of 100 Hz; 200 s long vibrations were simulated. Parameters used in this model are qualitative taken as $m = 1\,\text{kg}$, $\mu_1 = 0.3$, $\mu_2 = 0.1$, $\omega_1 = 1.73\,\text{Hz}$, $\omega_2 = 1\,\text{Hz}$, and $f = 50\,\text{N}$.

A sinusoidal excitation with the frequency of 4 Hz and the amplitude of 50 unit displacement was applied to the model. From the discussion in Sect. 2, we can learn that the solution of x_2 only contain the frequency content at the excitation frequency ω. Therefore, subharmonics will not occur in the response of x_2. Figure 2a shows the segmental time trace of x_1, and the received waveforms approximate to complete sinusoidal waves. Figure 2b shows the frequency-domain spectrum of x_1, from which one can notice the superharmonic components, but not the subharmonic component. This implies that the model encapsulates nonlinear characteristics and current excitation condition does not match the subharmonic generation requirements.

For the second numerical case study, a sinusoidal excitation with the frequency of 3.46 Hz ($2\omega_1$) and the amplitude of 50 unit displacement was applied to the model. Figure 3a shows a wave distortion of x_1, where the amplitude and shape of adjacent carriers become different compared with Fig. 2a, resulting in the doubling of the period. Figure 3b shows the frequency-domain spectrum of x_1. Compared with Fig. 2b, two additional peaks appeared, which can be identified as a subharmonic (1.73 Hz) and superharmonic (5.19 Hz) in Fig. 3.

Comparing Fig. 2b with Fig. 3b, it is found that superharmonic components occur in both response signals, which means the simplified bolted joint structure model is capable of capturing the nonlinearity due to bolt looseness. When the amplitude of the excitation exceeds a certain value and when the excitation frequency is close enough to twice the natural frequency, subharmonic component will generate stemming from the nonlinear term in Eq. (15) and as shown in Fig. 3b. Thus, these expressions give a theoretical basis and guidelines for the subharmonic resonance method for the detection of bolted joint looseness. Subharmonic component is not observed when the excitation frequency is tuned away from twice the natural frequency. This observation qualitatively verifies the analytical predictions presented in Sect. 2.

To have a better appreciation of the excitation condition for subharmonic resonance, the excitation frequency was tuned around twice the natural frequency to vary from 3.2 to 3.8 Hz with a step of 0.05 Hz and the excitation amplitude was tuned from 35 to 55 with a step of 2 unit displacement. The results with combinations various excitation frequencies and different excitation amplitudes were examined. Figure 4 presents the subharmonic resonance condition. The red dots denote the presence of subharmonic resonance under the corresponding excitation condition in the numerical

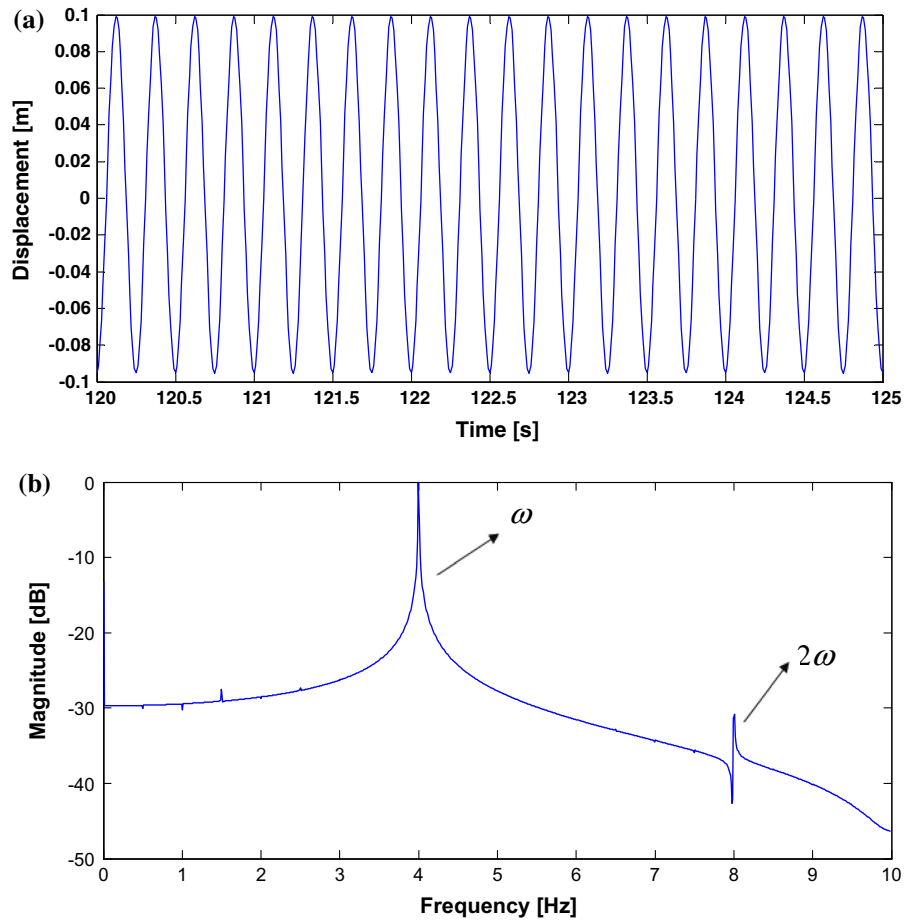

Fig. 2 The response of x_1 with excitation frequency at 4 Hz and the excitation amplitude of 50. **a** Time domain of response signal. **b** Frequency domain of response signal

results. The blue curve outlines the theoretical solution of Eq. (24). From Fig. 4, we can see that the theoretical solution agrees well the numerical simulation and the excitation frequency region of subharmonic resonance increases with the excitation amplitude.

4 Experiments

The experimental study aims to verify the simulation results demonstrating subharmonic resonance condition, as well as to show the validity of the subharmonic resonance damage identification method for bolt looseness detection. The experimental setup and the specimen are shown in Fig. 5. Two identical aluminum beams (400 mm long, 90 mm wide, and 2 mm thick) were connected at one of their free ends by a bolt. Two PZT active sensors with the diameter of 6.35 mm and thickness of 0.25 mm were surface-bonded on the aluminum beams, respectively, for actuation and sensing. The PZTs were placed with the distance of 120 mm away from the joint on each side. Sponges were used to support both ends of the beam to approximate free boundary conditions. A continuous sinusoidal signal generated by function generator (Agilent 33522A) was applied to the transmitter PZT through a linear power amplifier (TEGAM2350), and an oscilloscope (Agilent D50-X3014A) was connected to the receiver PZT to collect the response data.

The bolt was tightened to 4 Nm (damage) to represent a bolt loosening state. One longitudinal natural frequency of the bolted joint structure was identified at 36.4 kHz by measuring the amplitude peak via sweeping the structure with the excitation frequency from 20 to 40 kHz. First, the excitation frequency was tuned from 72 to 73 kHz with a step of 0.01 kHz, and the excitation amplitude was held at 100 Vpp. It was observed that the excitation frequency of 72.68–72.71 kHz can produce a subharmonic response. For the

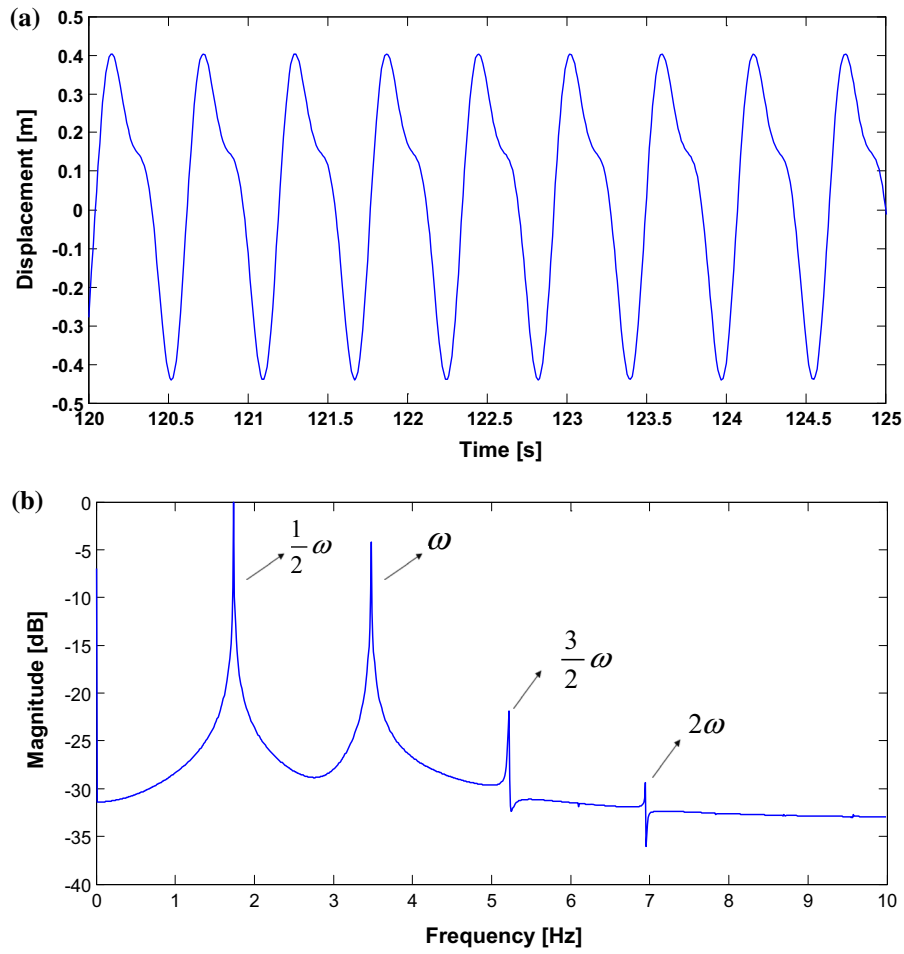

Fig. 3 The response of x_1 with excitation frequency 3.46 Hz and excitation amplitude 50. **a** Time-domain of response signal. **b** Frequency domain of response signal

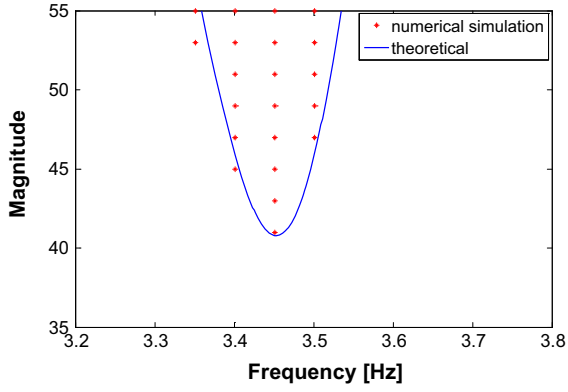

Fig. 4 Subharmonic resonance condition showing that the generation of subharmonic resonance posed a combination requirement on the excitation frequency and amplitude

purpose of demonstration, a 100 Vpp and 72.70 kHz sinusoidal excitation at a torque value of 4Nm was chosen as a showcase. The discrete Fourier transform was performed on the output signal. The corresponding response spectrum is shown in Fig. 6.

As shown in Fig. 6, the amplitudes of adjacent carriers became different, resulting in the doubling of the period and halving the frequency in the spectrum. Additional peaks appeared in the frequency-domain spectrum when exciting the loosening structure, identified as superharmonic components (2ω, 3ω) and subharmonic component ($1/2\omega$). Bolt looseness was assumed to be the main source of nonlinearity which generated these harmonic responses. This observation qualitatively verifies the results of the numerical simulation presented in Fig. 3.

Excitation amplitude was then increased to 150 Vpp, and the above operations were repeated. It was found that the excitation frequency of 72.67–72.72 kHz could produce a subharmonic response. A 150 Vpp and 72.70 kHz sinusoidal excitation was applied on the

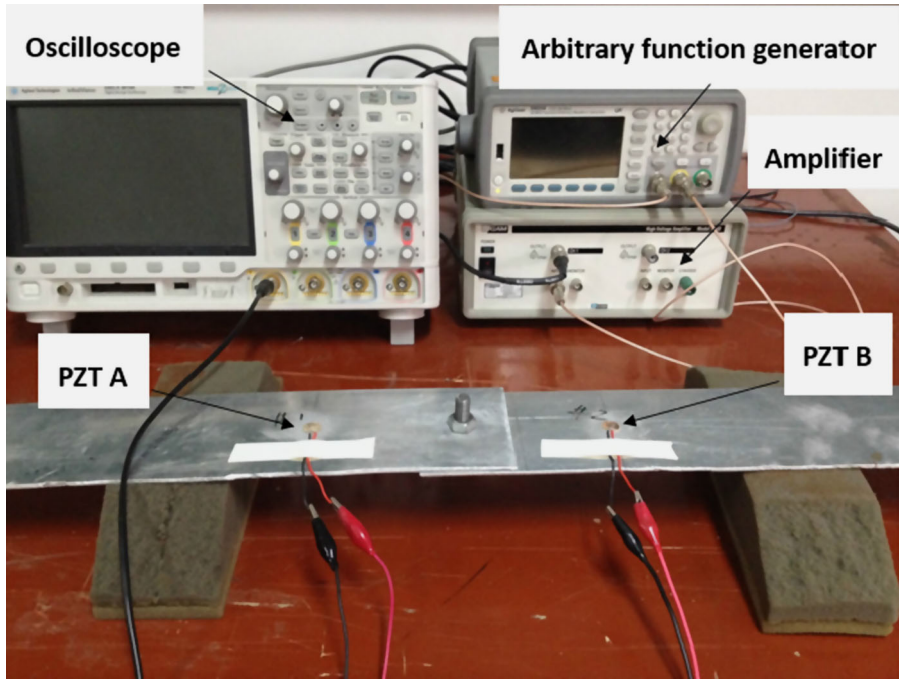

Fig. 5 Experimental setup of nonlinear subharmonic resonance method for the detection of bolt looseness with PZT active sensors

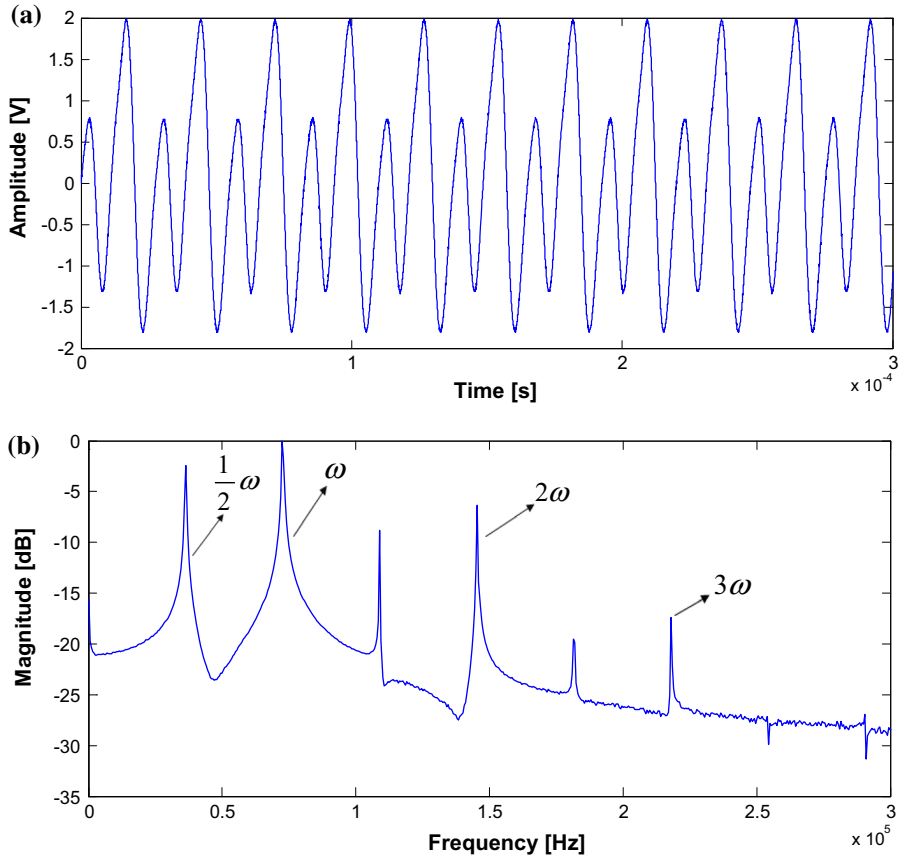

Fig. 6 Spectrum of sensing signal from the loose bolted joint (excitation frequency 72.70 kHz and excitation amplitude 100 Vpp). **a** Time domain of response signal. **b** Frequency domain of response signal

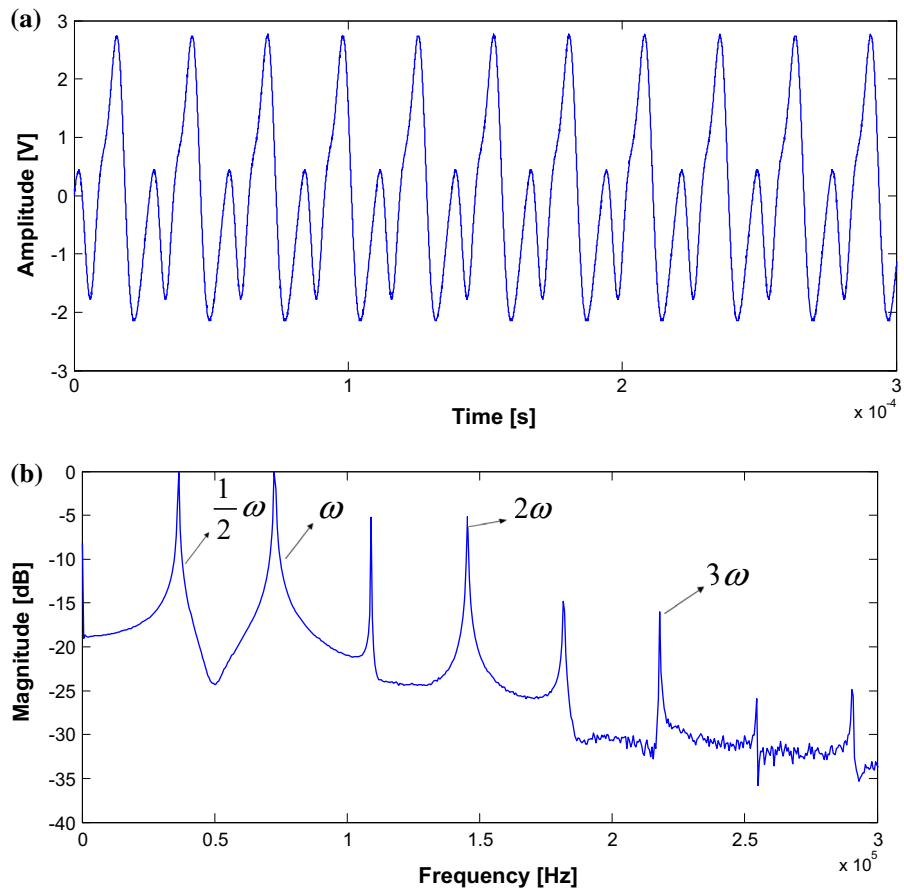

Fig. 7 Spectrum of sensing signal from the loose bolted joint (excitation frequency 72.70 kHz and excitation amplitude 150 Vpp). **a** Time domain of response signal. **b** Frequency domain of response signal

transmitter PZT as an illustrative showcase. Figure 7 shows the corresponding response spectrum.

As shown in Fig. 7, waveforms in time domain were similar to Fig. 6a. Superharmonic components $(2\omega, 3\omega)$ and subharmonic component $(1/2\omega)$ were also observed in the frequency-domain spectrum. From Sect. 3, we concluded that excitation frequency region of subharmonic resonance would increase with a larger excitation amplitude. Experimental results showed that with the excitation amplitude increasing from 100 to 150 Vpp, the range of subharmonic resonance indeed has increased (from 72.68–72.71 kHz to 72.67–72.72 kHz).

To demonstrate the effectiveness of the proposed bolt loosening detection approach using the subharmonic resonance, the bolt torque was tightened to 24 Nm which corresponds to a healthy condition. The above operations were repeated with the excitation amplitude of 150 Vpp. For this healthy case, the subharmonic component was not observed when the excitation frequency was tuned from 72 to 73 kHz. As a showcase, a 150 Vpp, 72.70 kHz sinusoidal excitation was applied on the transmitter PZT. Figure 8 shows the corresponding response spectrum.

It can be noticed from Fig. 8 that when the bolted joint was in healthy condition, there would approximate the waveform of sinusoidal waves in time domain; no subharmonic component was observed in the frequency-domain spectrum. However, considerable participation of superharmonic components $(2\omega, 3\omega)$ was observed in the response spectrum which means the bolt looseness is not the only source of nonlinearity in a practical testing. Thus, it is more convincing and reliable to detect nonlinear damage by analyzing the subharmonic component in frequency-domain spectrum, rather than the superharmonic components. In other words, superharmonic components appeared in both damaged and health conditions. It seems that these components can be identified as interfering signals which would appear inevitably whether the bolted

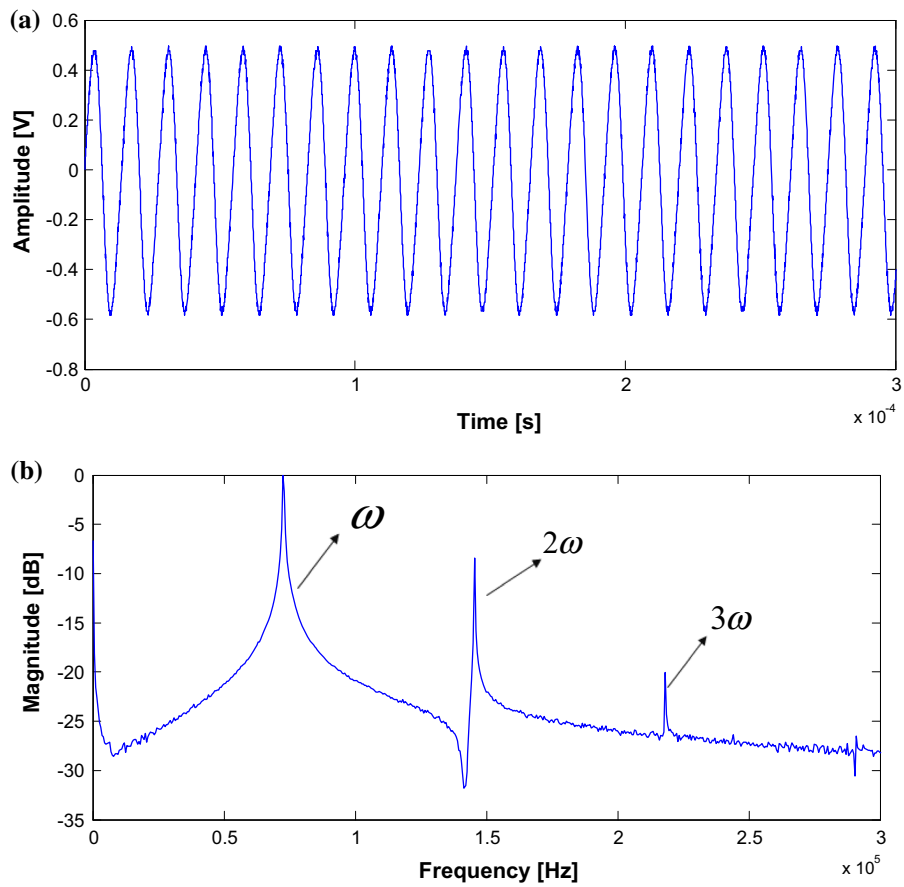

Fig. 8 Spectrum of sensing signal from the tight bolted joint (excitation frequency 72.69 kHz and excitation amplitude 150 Vpp). **a** Time domain of response signal. **b** Frequency domain of response signal

joint is tight or not. Therefore, harmonic methods of nonlinear ultrasonic testing are adversely affected by the measuring equipment nonlinearity and prone to lead false alarm of damage identification. Comparing Fig. 7 with Fig. 8, it was found that although identical excitation was applied on the loosening and healthy structure, yet the subharmonic component only appeared in the response of the loosening structure. This implies that nonlinearity caused by structural damage is the internal factor of producing subharmonics. Comparing these three groups of experiments, it was found that the generation of subharmonic requires particular conditions on input signal when the bolt becomes loose. Such a condition for producing subharmonics was found using the method of multiple timescales on a 2-DOF nonlinear model in Sect. 2. To trigger subharmonic resonance, the system must be excited at its subharmonic resonance region, which looks like a V-shape. It implies that the threshold of excitation amplitude reaches its minimum when the excitation frequency is around twice the natural frequency. And higher excitation is required, while the excitation frequency shifts away from twice the natural frequency. Such a threshold behavior makes the subharmonic methods more suitable for bolt loosening detection for bolted joint structures. And subharmonic methods can detect bolt looseness without the influence from equipment nonlinearity overcoming the limitation and difficulties of harmonic methods.

5 Conclusion

A 2-DOF nonlinear model simulating the bolted joint structure was proposed to investigate the excitation condition on subharmonic resonance. Conditions for the subharmonic resonance generation were found theoretically with respect to the excitation frequency and the excitation amplitude. Both analytical prediction and numerical simulations were carried out to verify the validity of the loosening detection method for bolted joint structures using the subharmonic resonance. The experimental data showed that subharmonic compo-

nents would occur in the response subjected to excitation frequency around twice the system natural frequency, where the threshold value of excitation amplitude reaches its minimum. Subharmonic methods can overcome the influence of equipment nonlinearity and can be used as an effective means for the detection of nonlinear damage caused by bolt looseness.

Acknowledgements Support from National Natural Science Foundation of China #51378402 and #51605284 is thankfully acknowledged.

References

1. Mínguez, J.M., Vogwell, J.: Effect of torque tightening on the fatigue strength of bolted joints. Eng. Fail. Anal. **13**(8), 1410–1421 (2006)
2. Meo, M., Zumpano, G.: Nonlinear elastic wave spectroscopy identification of impact damage on a sandwich plate. Compos. Struct. **71**, 469–474 (2005)
3. Solodov, I., Pfleiderer, K., Busse, G.: Nonlinear Acoustic NDE: Inherent Potential of Complete Nonclassical Spectra. In: Universality of Nonclassical Nonlinearity, pp. 467–486 (2006)
4. Coelho, C.K., Das, S., Chattopadhyay, A., et al.: Detection of fatigue cracks and torque loss in bolted joints. In: Proceedings of Spie, 6532 (2007)
5. Liang Y., Zhang Y. C., Ding K. Q., et al.: Monitoring and Localization of Loosened Bolts Based on E/M Impedance Method. Sci. Technol. Eng. **13**(18), 1671–1815 (2013)
6. Argatov, I., Sevostianov, I.: Health monitoring of bolted joints via electrical conductivity measurements. Int. J. Eng. Sci. **48**(10), 874–887 (2010)
7. Jalali, H., Ahmadian, H., Mottershead, J.E.: Identification of nonlinear bolted lap-joint parameters by force-state mapping. Int. J. Solids Struct. **44**(25–26), 8087–8105 (2007)
8. Eriten, Melih, Kurt, Mehmet, Luo, Guanyang, et al.: Nonlinear system identification of frictional effects in a beam with a bolted joint connection. Mech. Syst. Signal Process. **39**(1–2), 245–264 (2013)
9. Amerini, F., Meo, M.: Structural health monitoring of bolted joints using linear and nonlinear acoustic/ultrasound methods. Struct. Health Monit. **10**(6), 659–672 (2011)
10. Fierro, G.P.M., Meo, M.: Residual fatigue life estimation using a nonlinear ultrasound modulation method. Smart Mater. Struct. **24**(2), 025040-238 (2015)
11. Jaques J., Adams D.: Using Impact Modulation to Identify Loose Bolts on a Satellite (2011)
12. Liu, S., Croxford, A.J., Neild, S., et al.: Effects of experimental variables on the nonlinear harmonic generation technique. IEEE Trans. Ultrason. Ferroelectr. Freq. Control **58**(7), 1442–1451 (2011)
13. Ohara, Y., Yamamoto, S., Mihara, T., et al.: Ultrasonic evaluation of closed cracks using subharmonic phased array. Jpn. J. Appl. Phys. **47**, 3908 (2008)
14. Johnson, D.R., Wang, K.W., Kim, J.S.: Investigation of the threshold behavior of subharmonics for damage detection of a structure with a breathing crack. In: SPIE Smart Structures and Materials+ Nondestructive Evaluation and Health Monitoring. International Society for Optics and Photonics, pp. 765032-9 (2010)
15. Mahmoodi, S.N., Jalili, N., Ahmadian, M.: Subharmonics analysis of nonlinear flexural vibrations of piezoelectrically actuated microcantilevers. Nonlinear Dyn. **59**(3), 397–409 (2010)
16. Bograd, S., Reuss, P., Schmidt, A., et al.: Modeling the dynamics of mechanical joints. Mech. Syst. Signal Process. **25**(8), 2801–2826 (2011)
17. Meyer, J.J., Adams, D.E.: Theoretical and experimental evidence for using impact modulation to assess bolted joints. Nonlinear Dyn. **81**(1–2), 103–117 (2015)
18. Nayfeh, A.H., Mook, D.T.: Nonlinear Oscillations. Wiley, New York (1979)